Environmental Pollution 227 (2017) 83–88

Contents lists available at ScienceDirect

Environmental Pollution

journal homepage: www.elsevier.com/locate/envpol

Mercury speciation in *Pinus nigra* barks from Monte Amiata (Italy): An X-ray absorption spectroscopy study☆

Laura Chiarantini [a], Valentina Rimondi [a], Fabrizio Bardelli [b, *], Marco Benvenuti [a], Claudia Cosio [c], Pilario Costagliola [a], Francesco Di Benedetto [a], Pierfranco Lattanzi [d], Géraldine Sarret [e]

[a] Dipartimento di Scienze della Terra, Università di Firenze, Via G. La Pira, 4, 50121 Firenze, Italy
[b] CNR-Nanotec c/o Dipartimento di Fisica, Università La Sapienza, P.le Aldo Moro 2, 00185, Roma, Italy
[c] Department F.-A. Forel for Environmental and Aquatic Sciences, Earth and Environmental Sciences, University of Geneva, 66 bd Carl-Vogt, CH-1211 Geneva 4, Switzerland
[d] CNR IGG, Istituto di Geoscienze e Georisorse, Via G. La Pira, 4, 50121 Firenze, Italy
[e] ISTerre, Univ. Grenoble Alpes & CNRS, 38058 Grenoble Cedex 9, France

ARTICLE INFO

Article history:
Received 27 February 2017
Received in revised form
7 April 2017
Accepted 17 April 2017

ABSTRACT

This study determined, by means of X-ray absorption near-edge structure (XANES) spectroscopy, the speciation of mercury (Hg) in black pine (*Pinus nigra*) barks from Monte Amiata, that were previously shown to contain exceptionally high (up to some mg kg^{-1}) Hg contents because of the proximity to the former Hg mines and roasting plants. Linear fit combination (LCF) analysis of the experimental spectra compared to a large set of reference compounds showed that all spectra can be fitted by only four species: β-HgS (metacinnabar), Hg-cysteine, Hg bound to tannic acid, and Hg^0. The first two are more widespread, whereas the last two occur in one sample only; the contribution of organic species is higher in deeper layers of barks than in the outermost ones. We interpret these results to suggest that, during interaction of barks with airborne Hg, the metal is initially mechanically captured at the bark surface as particulate, or physically adsorbed as gaseous species, but eventually a stable chemical bond is established with organic ligands of the substrate. As a consequence, we suggest that deep bark Hg may be a good proxy for long term time-integrated exposure, while surface bark Hg is more important for recording short term events near Hg point sources.

1. Introduction

Tree barks are, in principle, excellent adsorbents of airborne pollutants, including toxic metals (Panichev and McCrindle, 2004; Baltrénaité et al., 2014). Due to its porosity, and to the lack of metabolic processes, bark surface was generally considered chemically inert (e.g. Schulz et al., 1999), i.e. with little or no capability to react in the presence of inorganic and organic substances. In spite of these potential advantages, until recently the use of tree barks for environmental monitoring was not widespread. Possible drawbacks for the employment of barks include a) low levels of pollutant accumulation, making analysis comparatively difficult; b) superposition of direct uptake from the atmosphere and metabolic uptake from soil via the root-phloem-xylem system (Lodenius, 2013). However, Chiarantini et al. (2016) showed the use of Hg concentrations in tree bark as a reliable biomonitor for Hg in an area of past Hg mining. Alternatively, the use of lichens for environmental monitoring is more widespread (e.g., Szczepaniak and Biziuk, 2003; Grangeon et al., 2012). However, this technique also has some disadvantages, including patchy distribution, slow regeneration rates, and difficulty in differentiating between similar species (Pacheco et al., 2002). By contrast, tree barks offer advantages such as year-round and ubiquitous availability, simple species identification, and easy sampling. Specifically for Hg, barks are a potentially ideal trap to monitor airborne pollution, since this metal is not significantly taken up through plant roots due to its low bioavailability in soils (Boszke et al., 2008). Mercury is a global pollutant (Selin, 2009), characterized by long residence times in the

☆ This paper has been recommended for acceptance by Prof. W. Wen-Xiong.
* Corresponding author.
E-mail address: fabrizio.bardelli@gmail.com (F. Bardelli).

http://dx.doi.org/10.1016/j.envpol.2017.04.038
0269-7491/

atmosphere, and a corresponding ability to be transported over long distances. An effective monitoring of its distribution patterns at regional scale would benefit from simple, low-cost techniques such as tree bark sampling.

Our research group recently documented comparatively high (several mg kg^{-1}) Hg concentrations in *Pinus nigra* barks from the Abbadia San Salvatore (Monte Amiata, Italy) Hg mine site (ASSM; Chiarantini et al., 2016). These high concentrations support the idea that the terrestrial vegetative biomass is, with soils, the primary reservoir of Hg derived from both natural and anthropogenic sources (Gamby et al., 2015). Leaves are considered to be a trap for Hg but, as suggested by Chiarantini et al. (2016), barks may also actively sequester this metal in significant amounts, contributing to its mass budget in forested areas. The mechanisms of Hg sequestration and the stability of its compounds in the bark tissues are key factors in controlling this budget, and for environmental biomonitoring purposes. To our knowledge, however, papers describing the speciation of Hg in barks are limited to the study conducted by Vázquez et al. (2002), who propose procyanidin as the most likely binder. Until recently, the reported Hg concentrations in barks (typically up to some tens of μg kg^{-1}; Siwik et al., 2010) were too low to encourage specific investigation on Hg speciation in this type of matrix. The concentrations reported by Chiarantini et al. (2016) are high enough to allow the determination of Hg speciation using X-ray Absorption Spectroscopy (XAS), and this study was carried out on a subset of the samples examined in the Chiarantini et al. (2016) study.

The Monte Amiata area is highly anomalous in Hg because of the presence of the 3rd largest Hg mine district in the world (Rimondi et al., 2015). Over a century of mining and roasting caused Hg dispersion in the atmosphere and in the drainage network. Moreover, the area hosts a geothermal field, which is exploited for the production of energy; geothermal power plants are an additional source of Hg in the environment (Bravi and Basosi, 2014). In the study by Chiarantini et al. (2016), barks of *Pinus nigra* were used as biomonitors of airborne Hg pollution of the area. Nevertheless the fate and form of Hg in bark remain unknown, and a better knowledge of those is needed to successfully implement the biomonitoring approach.

The objective of this study is to improve our understanding of the uptake of Hg by barks. More specifically, we seek to determine the partitioning and fate of Hg in the surface and in deeper compartments of barks. To this end, we studied *Pinus nigra* barks from ASSM by X-ray absorption near-edge structure (XANES) spectroscopy. The study was conducted on a limited number of samples, and the results are therefore exploratory; nonetheless, we believe that they are useful for understanding the nature and dynamic of interaction between airborne Hg and tree barks, and to further use barks for Hg biomonitoring.

2. Materials and methods

Samples were recovered as five-centimeter thick cylinders using a hand-drill from trees close to the ASSM, to the geothermal power plants at Piancastagnaio, and from sites far from any known anthropogenic source, representing the local natural background (Fig. 1).

The choice of sites was aided by data on air Hg^0 concentrations (ng m^{-3}), as reported by Vaselli et al. (2013) and Cabassi et al. (2017), and summarized in Table 1.

Bark sampling was carried out at a height of about 1.5 m above the ground, selecting trees having approximately the same size (about 35 cm trunk radius, measured at a height of 60 cm above ground level) and age (around 60 years; S. Visconti, personal comm.). Bark grow rates are poorly known, therefore we cannot specify the ages of single bark layers.

Barks of the *Pinus* genus, in particular the *P. nigra* species, usually consist of stratified bark sheets, each having a thickness of 1–2 mm. These sheets can be easily separated from one another. Barks were dissected into several (three to seven) layers at increasing depth from the surface exposed to air. The position of a given slice within the bark core was identified, measuring the distance (mm) from the external surface exposed to the atmosphere as indicated in Table 1.

Mercury content was determined by DMA (Direct Hg analyzer), as described in Chiarantini et al. (2016). The highest Hg contents (up to 8.6 mg kg^{-1}) were found in samples close to the former mining area; samples close to geothermal plants showed much lower values (maximum 0.12 mg kg^{-1}), comparable to local background values. Across the bark thickness, Hg contents showed a general decrease from the first two layers to the innermost layers but, in some barks from highly polluted sites, Hg reaches its maximum concentration at 10–20 mm below the bark surface rather than at the bark-air interface (see Fig. 3 in Chiarantini et al., 2016).

For this study, we selected some trees already studied by Chiarantini et al. (2016): three samples from sites closest to the ASSM (PC8; PC13; PC17), two from sites close to geothermal power plants (PC4; PC2), plus a sample considered representative of the local natural background (PC 25) (Fig. 1); for all samples, the outermost layer was considered (0.2 mm beneath the surface), but for two of the ASSM samples we also included an intermediate layer (8–16 mm) (Table 1).

Thus, in total, eight bark samples were analyzed, each representing a specific layer of a sampled tree; the number was dictated by the long acquisition times required for high quality spectra at high Hg dilution level, and the limited beamtime available. The actual Hg content of sample portions (about 0.5 g) brought to the beamline was specifically determined (see Chiarantini et al., 2016 for details of the procedure).

Tree bark samples were reduced in fine powders to achieve higher homogeneity, and then pressed into self-supporting pellets of 5 mm diameter for XAS measurements. Extreme care was taken to avoid cross contamination among samples having different concentrations.

XAS measurements at the Hg L_{III}-edge (12.284 keV) were performed at the European Radiation Synchrotron Facility (ESRF, Grenoble, France) using the bending magnet French absorption spectroscopy beamline (FAME-BM30B, Proux et al., 2005, 2006; Hazemann et al., 2009). Two Rh-coated mirrors, located before and after the monochromator with respect to the beam direction, were used for efficient harmonics rejection, collimation, and vertical focusing of the beam. A sagittal focusing system provided a beam intensity of 10^{10} photons s^{-1} at 12 keV, and a beam size on the sample of approximately 300 × 200 μm (H × V). The beam energy was selected using a couple of Si (220) crystals; at the working energy and conditions, the energy resolution is estimated to be ~0.5 eV. A Hg^0 reference, prepared by mixing elemental Hg in epoxy resin as described in Rimondi et al. (2014), was used to calibrate the monochromator energy. Due to the high dilution level of the absorber element (Hg), near-edge (XANES) spectra of the tree bark samples were recorded in fluorescence mode using a high-throughput 30-element solid state Ge detector (Canberra, St Quentin Yvelines, France). Conversely, concentrated Hg reference compounds were acquired in transmission mode using two ionization chambers to measure the incoming and transmitted X-ray beam. All samples and references investigated in this study were analyzed at 20 K, to avoid possible beam-induced redox reactions, which could have altered their speciation. Particular attention was devoted to keep oxygen-sensitive references in anaerobic environment until measurements. Typically, nine to eleven 30-min

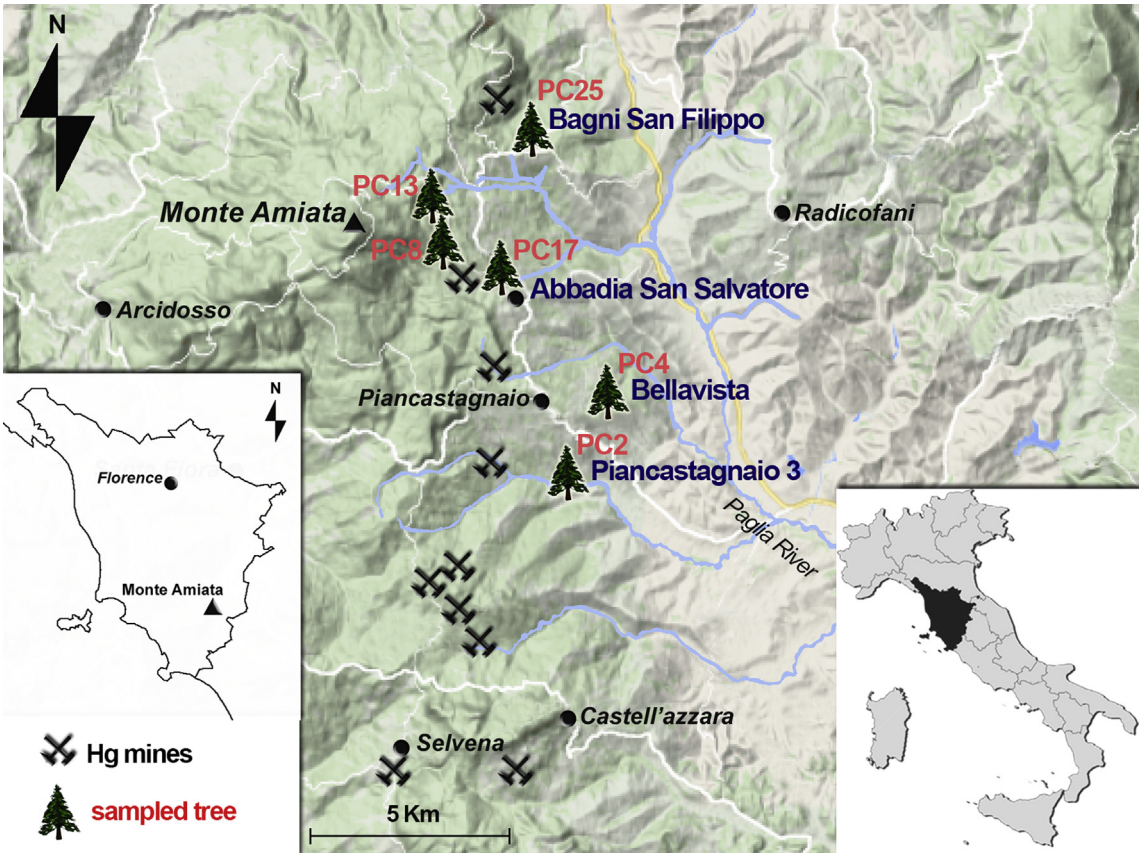

Fig. 1. Map of the Monte Amiata Hg mining district with the location of exploited Hg mines in the region (crossed hammers) and sampling sites (tree symbols) selected for barks of *Pinus nigra*; symbols: black dots = towns; black triangle: mountain peak (after Chiarantini et al., 2016).

Table 1
List of analyzed tree bark samples.

Sample	Hg content (mg kg^{-1})	Notes	Location	Air Hg^0 content (ng m^{-3})
PC8_1	3.20	outermost layer (0–2 mm)	Abbadia San Salvatore mine site (ASSM)	735[a]
PC8_2	6.82	intermediate layer (6–8 mm)	Abbadia San Salvatore mine site (ASSM)	735[a]
PC13_1	2.65	outermost layer (0–2 mm)	Abbadia San Salvatore mine site (ASSM)	735[a]
PC17_1	5.00	outermost layer (0–2 mm)	Abbadia San Salvatore mine site (ASSM), urban area	450[a]
PC17_3	5.24	intermediate layer (14–16 mm)	Abbadia San Salvatore mine site (ASSM), urban area	450[a]
PC4_1[c]	0.10	outermost layer (0–2 mm)	Bellavista geothermal power plant	27–57[b]
PC2_1[c]	0.12	outermost layer (0–2 mm)	Piancastagnaio 3 geothermal power plant	27–57[b]
PC25_1[c]	0.80	outermost layer (0–2 mm)	Bagni S. Filippo (local natural background)	12[a]

[a] Average values as reported by Vaselli et al. (2013).
[b] Range of average values during 4 days of measurements as reported by Cabassi et al. (2017). Concentrations at each location are highly variable, mostly depending on atmospheric conditions; the values shown should be taken as order of magnitude.
[c] The spectra obtained were of insufficient quality, and are not shown here (see text).

consecutive scans were acquired for samples with concentrations > 1 mg kg^{-1}, for a total acquisition time of ~5 h per sample. For sub-ppm samples, eighteen to twenty-four 30-min consecutive scans were acquired, accounting for a total acquisition time of 9–12 h per sample. Three 30-min consecutive scans were acquired for the Hg-references. For all samples, no changes were observed in the spectral features of all consecutive scans, indicating that beam-induced reduction or oxidation did not occur. The XANES spectra were background subtracted and normalized, and energy calibrated using the spectrum of the Hg^0 reference placed behind the samples and measured along with the samples spectra.

The acquired spectra were analyzed by finger-print XANES analysis, and by semi-quantitative Linear Combination Fitting. This approach can allow revealing the speciation of Hg in the samples by comparison with a set of Hg references representative of the samples speciation. The samples speciation being of course unknown *a priori*, selecting the best candidate references is not a trivial task. For this reason, great care was paid to the choice of references, and many possible inorganic and organic Hg bonding environments were considered. These included: Hg sulfides, oxides, chlorides, as well as hydroxyls and carboxyls (tannic acid and cellulose), sulfur (thiols, sulfides, sulfates), methylate, and glutarate bondings. XANES spectra of the Hg references are presented as electronic supporting information (Figure S1).

Inorganic Hg references include: $HgCl_2$, Hg_2Cl_2, $HgSO_4$, HgO, which were synthetic chemicals purchased by Merck or Sigma

Aldrich (purity > 95%); α-HgS (cinnabar), and β-HgS (metacinnabar), natural specimens obtained from J.E. Gray, U.S. Geological Survey. These natural specimens were checked for purity by means of X-ray powder diffraction prior to include them in the reference set. These references were pressed to pellets after mixing the right amount of powder with cellulose to obtain a suitable absorption for XAS measurements.

Glutarate, cysteine, and diethylmaleate solutions were prepared as 200 mM solution by dissolution of powders (all from Sigma) in water. $HgCl_2$ and CH_3HgCl solutions were prepared at 5000 mg L^{-1} from powder (Sigma) in Milli-Q® water. The $HgCl_2$ solution was mixed with the glutarate, cysteine, or diethylmaleate solutions to obtain 60 mM Hg-glutarate, Hg-cysteine, or Hg-diethylmaleate solutions (final solutions were made by mixing 3 mL of the organic compound solution with 4 mL of Hg solution and 2.5 mL of glycerol, pH adjusted to 5, and final volume adjusted to 10 mL). The CH_3HgCl solution was mixed to the cysteine or diethylmaleate solutions to obtain 60 mM MeHg-cysteine or MeHg-diethylmaleate solutions in the same way as described above. All solutions were plunged in liquid nitrogen and then transferred in the cryostat for XAS measurements. The Hg-tannic acid reference was prepared by dissolving 500 mg of tannic acid in water, adding 2.5 mL of $Hg(NO_3)_2$ 1000 mg L^{-1} solution, adjusting the pH to 5.0, and then freeze drying the solution.

The cellulose references were prepared by mixing a solution of Hg^{2+} or CH_3Hg^+ (2000 or 6000 mg L^{-1}) with a water suspension (10 mL) of cellulose powder (150 mg) at pH 5. The Hg-cellulose or MeHg-cellulose references were then obtained upon centrifugation, and measured as humid pellets. All the references in solution and the Hg-cellulose references were recorded in fluorescence mode.

All possible combinations of two to five components linear combination fits were optimized by minimizing the reduced χ^2. Starting from the best two components fit, the best fit with $n + 1$ components was considered to be significantly better than the best n-component one, if a net decrease of 10–20% of its χ^2 was achieved. The precision of the fractions obtained from LCF was previously estimated to be between 10 and 20% of the total Hg content (Bardelli et al., 2011; Isaure et al., 2002), but it strongly depends on the signal to noise ratio. Fractions occurring in amounts <10% were found to improve the fits negligibly, and were therefore ignored. The sum of the fractions was comprised between 99 and 101% for all samples, supporting the correctness of the fitting procedure. Data treatment and linear combinations were performed using the IFEFFIT (Interactive XAFS analysis and FEFF fitting) software package (Ravel and Newville, 2005).

3. Results and discussion

All samples spectra, including those with the lowest Hg concentrations, showed a recognizable Hg L_{III} absorption edge step. However, only for the five samples with Hg > 1 mg kg^{-1} the signal to noise ratio was sufficiently high to allow a meaningful LCF analysis. The samples spectra with the corresponding LCF curves and the reference spectra are displayed in Fig. 2, whereas the results of LCF analysis are presented in Table 2.

For all spectra, a meaningful fit can be obtained by considering only four reference compounds: β-HgS (metacinnabar), Hg bound to tannic acid, or Hg cysteine, and Hg^0. We cannot rule out the presence of minor amounts of other compounds that cannot be identified by the LCF procedure. Among inorganic species, metacinnabar is ubiquitous, whereas Hg^0 was identified only in sample PC8_1, where the fit was found to improve significantly (>20%) by introducing 20% Hg^0, along with 80% metacinnabar. This sample is the closest to the former roasting area of ASSM, where the highest values of gaseous Hg were measured in the survey by Vaselli et al. (2013). For samples where two layers were analysed, the contribution of inorganic species markedly decreases from the outermost to the innermost layer.

Among organic species, Hg-cysteine is the most commonly found, especially in the internal layers (PC8_2 and PC17_3), although it also occurs as a major contributor in sample PC13_1; Hg bound to tannic acid was found as a minor contributor in one sample only (PC17_1).

Metacinnabar and Hg^0 most likely represent the original species deposited onto the barks by interaction with the surrounding atmosphere. Specifically, Hg^0 would be deposited directly from the atmosphere as an adsorbed gaseous species, as observed in a study concerning tree leaves in the USA (Laacouri et al., 2013), whereas metacinnabar likely represents wind-blown particulate from the surrounding soils and/or mine waste piles. Particulate is an important fraction of airborne Hg at mining sites (e.g., Moreno et al., 2005). In mine waste and contaminated sediments and soils, metacinnabar represents a major Hg compound, similar to other Hg districts (e.g., Esbrí et al., 2010; Rimondi et al., 2014 specifically for Monte Amiata). Metacinnabar is rare in the primary ore, but it widely occurs as a byproduct of the ore roasting process: when heated to >600 °C, cinnabar decomposes to Hg and S, and also generates residual metacinnabar (Kim et al., 2000). Moreover, metacinnabar, the most environmentally relevant HgS(s) compound (Drott et al., 2013), can form in soil and sediments under anoxic conditions. In barks, the absence of cinnabar (at least, in amounts identifiable by XANES), which is equally present in waste piles, soils and sediments at Monte Amiata (Rimondi et al., 2014), is unclear. Possible, albeit not conclusive, explanations include the following: because of the above mentioned formation during ore roasting, metacinnabar is especially abundant in calcines (residues of ore roasting), typically consisting of very fine-grained material (Kim et al., 2000). Hence we suggest a dominant contribution of calcines to particulate airborne Hg (see also Yin et al., 2013); metacinnabar is slightly less dense than cinnabar (7.8 vs. 8.2 g cm^{-3}), and could be preferentially transported in the particulate.

Conversely, it is also known that some plants may synthesize metacinnabar inside their tissues, as shown in the roots of an aquatic plant (Cosio et al., 2014). In principle, one could speculate that metacinnabar in the barks could be a newly formed phase resulting from an unknown metabolic process. However, we believe that this possibility is unlikely. Metacinnabar is especially abundant in the outermost layers, i.e. in direct contact with the oxidizing atmosphere environment, where sulfide formation should not be favored. Moreover, if this phase were the result of a biological process, we would expect finding it especially in the innermost layers, which is not the case here.

For similar reasons, we take the presence of organic-bound Hg as an indication of an interaction between the deposited inorganic species and the biological substrate. Organic-bound Hg may be present in the surrounding soils, but it is a comparatively minor fraction of the total Hg (Malferrari et al., 2011; Rimondi et al., 2014). Moreover, if organic-bound Hg in the barks were mostly derived from soil particulate, its presence should be enhanced in the outermost layers, and not vice versa. Specifically, the contribution of the Hg cysteine spectrum to the LCF certainly indicates the presence of Hg bound to thiol groups, while the contribution of Hg-tannic acid may be attributed to the presence of Hg bound to polyphenolic compounds and supporting tissues. The affinity of Hg with bark tannins was suggested by Vázquez et al. (2002) to explain the ability of barks to remove Hg ions from aqueous solutions. On the other hand, the affinity of Hg with “soft” donors like thiols is well established (e.g. Riccardi et al., 2013), and is well compatible with the establishment of bonds with –SH groups in cysteine-like

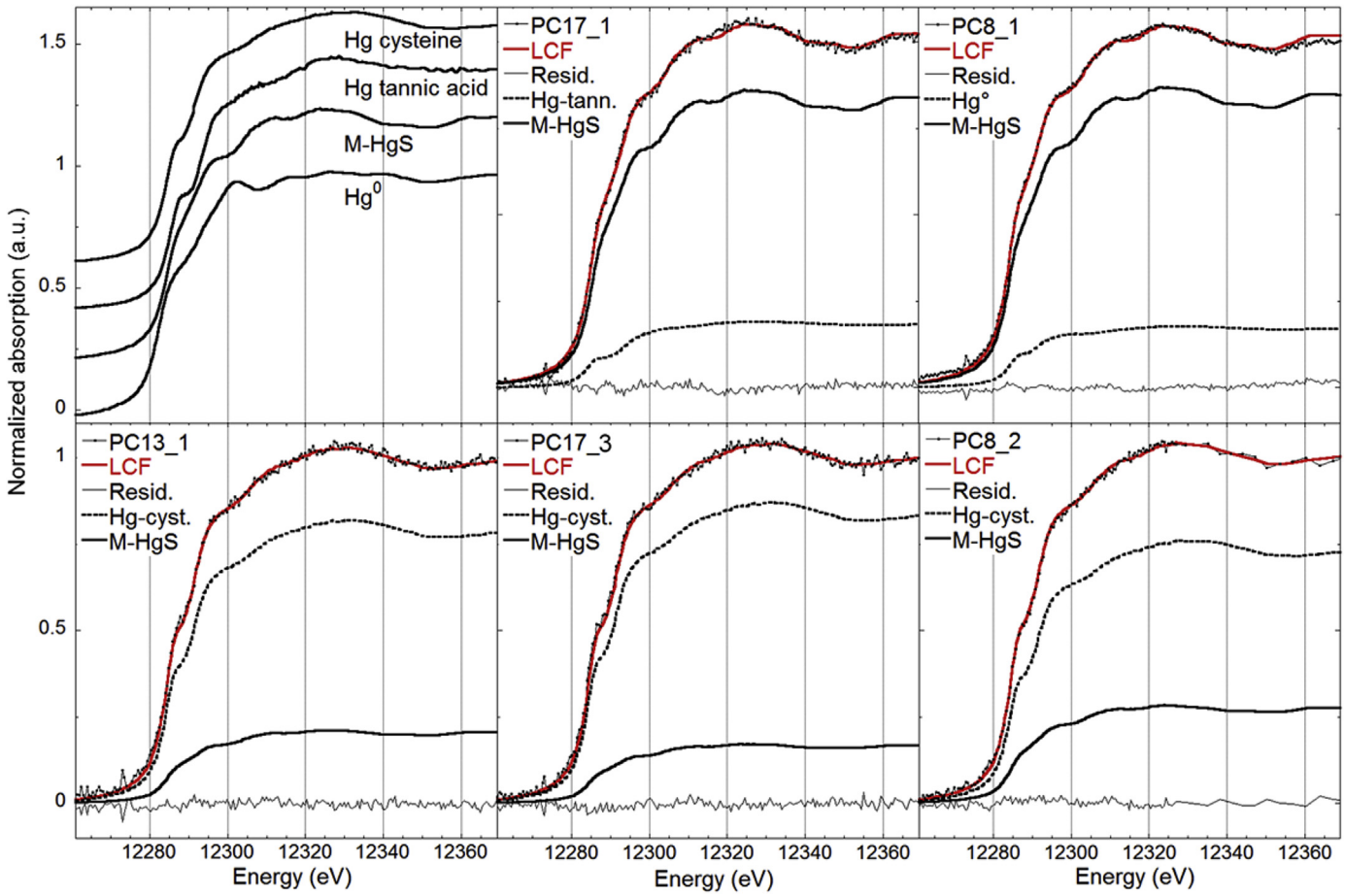

Fig. 2. XANES spectra of the references used to perform linear combination fits (upper left panel). Only the references that contributed significantly to the LCF are shown. The other panels show the spectra of bark samples from ASSM. The spectra are reported with the fit curves (LCF) superimposed, the fractions of the references used in the LCF (as reported in Table 2), and the residuals (i.e. the difference between the sample spectrum and the fit). M-HgS: metacinnabar; Resid: residual; Hg-cyst.: Hg-cysteine; Hg°: elemental Hg.

Table 2
Results of LCF analysis. The sum of the fractions (%) and the reduced χ^2 values are also reported. The reported errors on the fractions are the ones generated by the IFEFFIT software, and are consistent with the observation that contributions of species lower than 10–15% improve the fits negligibly.

Sample	Hg-cyst %	Hg-tannic %	β-HgS %	Hg^0%	Σ	$\chi^2.10^4$
PC13_1	77 ± 4		22 ± 4		99	1.4
PC17_1		20 ± 3	82 ± 3		101	1.2
PC17_3	84 ± 4		16 ± 4		100	0.9
PC8_1			83 ± 2	18 ± 2	100	0.9
PC8_2	74 ± 5		26 ± 5		100	0.9

molecules. In short, Hg seems to be retained in barks mostly by complexation with thiol-containing proteins and peptides (which could be, among others, extensin and glutathione), and subordinately with COOH and OH groups of tannins. Considering the total Hg amounts in the samples (Table 1), and the proportions of organic-bound Hg (Table 2), up to 4.5 mg kg^{-1} Hg may be present as organic complexes.

As already suggested by Chiarantini et al. (2016), this study confirmed that Hg can be effectively retained by *Pinus nigra* barks through atmospheric deposition, with minor systemic uptake from soils. Considering a Hg average content in tree bark of 1 mg kg^{-1} (mean value from Chiarantini et al., 2016) and a mean bark density of 400 kg m^{-3} (Miles and Smith, 2009), we estimated that a tree of 10 m height (35 cm of radius) could entrap about 250 mg of Hg in 3 cm of bark thickness, acting as an efficient sink for Hg. Moreover, we firstly demonstrate that barks do not simply behave as passive, inert surface for Hg deposition, but they do have an active role in Hg entrapment, through complexation with the organic matter.

Mercury entrapment by atmospheric deposition represents the preliminary condition to propose barks as efficient biomonitors. However, one of the major points to be clarified is how permanently Hg can reside in barks and how long barks could be exposed to pollutants during their growing cycle. Mercury chemical speciation, bark composition, and age are probably the most relevant factors that may influence Hg binding to the bark substrate. An ongoing project specifically aimed at age determination of the different bark layers will hopefully offer a further opportunity to investigate the processes controlling Hg speciation at the bark interface.

4. Conclusions

This study investigates the speciation of Hg in *Pinus nigra* barks from the Monte Amiata region (Italy) by means of X-ray absorption spectroscopy (specifically, XANES). The barks are exceptionally rich in Hg because of the proximity to wastes of the former mines and production facilities. Linear combination fitting of experimental XANES spectra to those of selected relevant reference Hg compounds suggests that Hg in these barks is partly present as inorganic species (mainly metacinnabar, and subordinately elemental

Hg), and partly bound to thiol-containing molecules or tannins. The organic-bound fraction markedly increases from the outermost bark layer to deeper layers.

This study strengthens the conclusions by Chiarantini et al. (2016), adding further support to the concept that tree barks, and specifically *Pinus nigra* barks, may represent suitable tools for monitoring airborne Hg. The Hg speciation data presented here for tree bark provide evidence of Hg dynamics and fate of Hg in bark: initially, the metal is mechanically captured at the bark surface as particulate, or physically adsorbed as gaseous species, but eventually a stable chemical bond is established with organic ligands of the substrate. As a consequence, we suggest that deep bark Hg may be a long term, time integrated proxy for Hg exposure, while surface bark Hg is more important for short term monitoring near Hg point sources.

Acknowledgments

The research was funded by MIUR (PRIN 2010-2011 and 2010MKHT9B grant to PC), University of Firenze ("ex-60%" grants to PC and FDB), and Regione Sardegna (LR7/2007 grant to PL). XANES spectra collection was made possible by ESRF support (experiments EV-165 and ES-126).

We thank the BM30B (Fame) beamline staff for technical support, and Alejandro Fernandez-Martinez for having prepared the Hg-tannic acid reference. We acknowledge the constructive criticism of two anonymous referees.

ISTerre is part of Labex OSUG@2020 (ANR10 LABX56).

Appendix A. Supplementary data

Supplementary data related to this article can be found at http://dx.doi.org/10.1016/j.envpol.2017.04.038.

References

Baltrénaité, E., Baltrénas, P., Lietuvninkas, A., Šerevičienė, V., Zuokaitė, E., 2014. Integrated evaluation of aerogenic pollution by air-transported heavy metals (Pb, Cd, Ni, Zn, Mn and Cu) in the analysis of the main deposit media. Environ. Sci. Pollut. Res. 21, 299–313.

Bardelli, F., Cattaruzza, E., Gonella, F., Rampazzo, G., Valotto, G., 2011. Characterization of road dust collected in Traforo del San Bernardo highway tunnel: Fe and Mn speciation. Atmos. Environ. 45, 6459–6468.

Bravi, M., Basosi, R., 2014. Environmental impact of electricity from selected geothermal power plants in Italy. J. Clean. Prod. 66, 301–308.

Boszke, L., Kowalski, A., Astel, A., Barański, A., Gworek, B., Siepak, J., 2008. Mercury mobility and bioavailability in soil from contaminated area. Environ. Geol. 55, 1075–1087.

Chiarantini, L., Rimondi, V., Benvenuti, M., Beutel, M., Costagliola, P., Gonnelli, C., Lattanzi, P., Paolieri, M., 2016. Black pine (*Pinus nigra*) barks as biomonitors of airborne mercury pollution. Sci. Total Environ. 569–570, 105–113.

Cabassi, J., Tassi, F., Venturi, S., Calabrese, S., Capecchiacci, F., D'Alessandro, W., Vaselli, O., 2017. A new approach for the measurement of gaseous elemental mercury (GEM) and H_2S in air from anthropogenic and natural sources: examples from Mt. Amiata (Siena, Central Italy) and Solfatara Crater (Campi Flegrei, Southern Italy). J. Geochem. Explor. 175, 48–58.

Cosio, C., Flück, R., Regier, N., Slaveykova, V.I., 2014. Effects of macrophytes on the fate of mercury in aquatic systems. Environ. Toxicol. Chem. 33 (6), 1225–1237.

Drott, A., Björn, E., Bouchet, S., Skyllberg, U., 2013. Refining thermodynamic constants for mercury(II)-sulfides in equilibrium with metacinnabar at submicromolar aqueous sulfide concentrations. Environ. Sci. Technol. 47, 4197–4203.

Esbrí, J.M., Bernaus, A., Ávila, M., Kocman, D., García-Noguero, E.M., Guerrero, B., Gaona, X., Álvarez, R., Perez-Gonzalez, G., Valiente, M., Higueras, P., Horvat, M., Loredo, J., 2010. XANES speciation of mercury in three mining districts – Almadén, Asturias (Spain), Idria (Slovenia). J. Synchrotron Radiat. 17, 179–186.

Gamby, R.L., Hammerschmidt, C.R., Costello, D.M., Lamborg, C.H., Runkle, J.R., 2015. Deforestation and cultivation mobilize mercury from topsoil. Sci. Total Environ. 532, 467–473.

Grangeon, S., Guedron, S., Asta, J., Sarret, G., Charlet, L., 2012. Lichen and soil as indicators of an atmospheric mercury contamination in the vicinity of a chlor-alkali plant (Grenoble, France). Ecol. Indic. 13, 178–183.

Hazemann, J.L., Proux, O., Nassif, V., Palancher, H., Lahera, E., Da Silva, C., Braillard, A., Testemale, D., Diot, M.A., Alliot, I., Del Net, W., Manceau, A., Gélébart, F., Morand, M., Dermigny, Q., Shukla, A., 2009. High-resolution spectroscopy on an X-ray absorption beamline. J. Synchrotron Radiat. 16, 283–292.

Isaure, M.P., Laboudigue, A., Manceau, A., Sarret, G., Tiffreau, C., Trocellier, P., Lamble, G., Hazemann, J.L., Chateigner, D., 2002. Quantitative Zn speciation in a contaminated dredged sediment by μ-PIXE, μ-SXRF, EXAFS spectroscopy and principal component analysis. Geochim. Cosmochim. Acta 9, 1549–1567.

Kim, C.S., Brown Jr., G.E., Rytuba, J.J., 2000. Characterization and speciation of mercury-bearing mine wastes using X-ray absorption spectroscopy (XAS). Sci. Total Environ. 261, 157–168.

Laacouri, A., Nater, E.A., Kolka, R.K., 2013. Distribution and uptake dynamics of mercury in leaves of common deciduous tree species in Minnesota. U.S.A. Environ. Sci. Technol. 47, 10462–10470.

Lodenius, M., 2013. Use of plants for biomonitoring of airborne mercury in contaminated areas. Environ. Res. 125, 113–123.

Malferrari, D., Brigatti, M.F., Elmi, C., Laurora, A., 2011. Determination of Hg binding forms in contaminated soils and sediments: state of the art and a case study approaching abandoned mercury mines from Mt. Amiata (Siena, Italy). N. Jb. Min. Abh 188/1, 65–74.

Miles, Patrick D., Smith, W. Brad, 2009. Specific Gravity and Other Properties of Wood and Bark for 156 Tree Species Found in North America. Res. Note NRS-38. U.S. Department of Agriculture, Forest Service, Northern Research Station, Newtown Square, PA, 35 pp.

Moreno, T., Higueras, P., Jones, T., McDonald, I., Gibbons, W., 2005. Size fractionation in mercury-bearing airborne particles (HgPM 10) at Almadén, Spain: implications for inhalation hazards around old mines. Atmos. Environ. 39, 6409–6419.

Pacheco, A.M.G., Barros, L.I.C., Freitas, M.C., Reis, M.A., Hipolito, C., Oliveira, O.R., 2002. An evaluation of olive-tree bark for the biological monitoring of airborne trace-elements at ground level. Environ. Pollut. 120, 79–86.

Panichev, N., McCrindle, R.I., 2004. The application of bio-indicators for the assessment of air pollution. J. Environ. Monit. 6, 121–123.

Proux, O., Biquard, X., Lahera, E., Menthonnex, J.J., Prat, A., Ulrich, O., Soldo, Y., Trévisson, P., Kapoujyan, G., Perroux, G., Taunier, P., Grand, D., Jeantet, P., Deleglize, M., Roux, J.P., Hazemann, J.L., 2005. FAME: a new beamline for X-ray absorption investigations of very-diluted systems of environmental, material & biological interests. Phys. Scr. 115, 970–973.

Proux, O., Nassif, V., Prat, A., Ulrich, O., Lahera, E., Biquard, X., Menthonnex, J.J., Hazemann, J.L., 2006. Feedback system of a liquid-nitrogen-cooled double-crystal monochromator: design and performances. J. Synchrotron Radiat. 13, 59–68.

Ravel, B., Newville, M., 2005. ATHENA, ARTEMIS, HEPHAESTUS: data analysis for X-ray absorption spectroscopy using IFEFFIT. J. Synchrotron Radiat. 12, 537–541.

Riccardi, D., Guo, H.B., Parks, J.M., Gu, B., Summers, A.O., Miller, S.M., Liang, L., Smith, J.C., 2013. Why mercury prefers soft ligands? J. Phys. Chem. Lett. 4, 2317–2322.

Rimondi, V., Bardelli, F., Benvenuti, M., Costagliola, P., Gray, J.E., Lattanzi, P., 2014. Mercury speciation in the Mt. Amiata mining district (Italy): interplay between urban activities and mercury contamination. Chem. Geol. 380, 110–118.

Rimondi, V., Chiarantini, L., Lattanzi, P., Benvenuti, M., Beutel, M., Colica, A., et al., 2015. Metallogeny, exploitation and environmental impact of the Mt. Amiata mercury ore district (southern Tuscany, Italy). Ital. J. Geosci. 134, 323–336.

Schulz, H., Popp, P., Huhn, G., Stärk, H.-J., Schüürmann, G., 1999. Biomonitoring of airborne inorganic and organic pollutants by means of pine tree barks. I. Temporal and spatial variations. Sci. Total Environ. 232, 49–58.

Selin, N., 2009. Global biogeochemical cycling of mercury: a review. Annu. Rev. Environ. Resour. 34, 43–63.

Siwik, E.I.H., Campbell, L.M., Mierle, G., 2010. Distribution and trends of mercury in deciduous tree cores. Environ. Pollut. 158, 2067–2073.

Szczepaniak, K., Biziuk, M., 2003. Aspects of the biomonitoring studies using mosses and lichens as indicators of metal pollution. Environ. Res. 93, 221–230.

Vaselli, O., Higueras, P., Nisi, B., Esbrí, J.M., Cabassi, J., Martinez-Coronado, A., et al., 2013. Distribution of gaseous Hg in the Mercury mining district of Mt. Amiata (Central Italy): a geochemical survey prior the reclamation project. Environ. Res. 125, 179–187.

Vázquez, G., González-Álvarez, J., Freire, S., López-Lorenzo, M., Antorrena, G., 2002. Removal of cadmium and mercury ions from aqueous solution by sorption on treated Pinus pinaster bark: kinetics and isotherms. Bioresour. Technol. 82, 247–251.

Yin, R., Feng, X., Wang, J., Bao, Z., Yu, B., Chen, J., 2013. Mercury speciation and mercury isotope fractionation during ore roasting process and their implication to source identification of downstream sediment in the Wanshan mercury mining area, SW China. Chem. Geol. 336, 72–79.